Journal of Molecular Catalysis A: Chemical 323 (2010) 1–6

Contents lists available at ScienceDirect

Journal of Molecular Catalysis A: Chemical

journal homepage: www.elsevier.com/locate/molcata

Editor Choice Paper

Effect of gallium as an additive in hydrodesulfurization WS_2/γ-Al_2O_3 catalysts

J.N. Díaz de León[a,b], M. Picquart[a], M. Villarroel[c], M. Vrinat[b], F.J. Gil Llambias[c], F. Murrieta[d], J.A. de los Reyes[a,*]

[a] Universidad A. Metropolitana-Iztapalapa, División de Ciencias Básicas e Ingeniería, Av. FFCC R Atlixco 186, Col. Vicentina, 09340 México, D.F., Mexico
[b] Institut de recherches sur la catalyse et l'environnement de Lyon, UMR 5256 CNRS-Université Lyon 1, 2 Av. Einstein 69626 Villeurbanne Cedex, France
[c] Universidad de Santiago de Chile, Departamento de Química, Santiago, Chile
[d] Instituto Mexicano del Petróleo, México, D.F., Mexico

ARTICLE INFO

Article history:
Received 21 November 2009
Received in revised form 3 March 2010
Accepted 3 March 2010
Available online 11 March 2010

Keywords:
Gallium
Tungsten sulfide
Hydrodesulfurization
Isoelectric point
Raman spectroscopy

ABSTRACT

The effect of gallium in W/Ga(x)–γ-Al_2O_3 catalysts was investigated in the hydrodesulfurization of dibenzothiophene. The γ-Al_2O_3 carrier was modified by the gallium addition prior to W impregnation and further calcination at 723 K. An electrophoretic study was carried out on the calcined Ga samples at 0, 0.29, 0.55, 0.84, 1.09, 1.43, 1.71 and 2.22 wt.% of Ga and it indicated that Ga addition affected significantly the surface of alumina. The presence of at least two gallium species was proposed, at low gallium content $GaAl_2O_4$ species decreased the isoelectric point (IEP) and probably the formation of Ga_2O_3 at higher contents increased again the IEP. Raman spectroscopy showed that the gallium incorporation had a strong effect in the formation of WO_x species at the surface of catalysts. The highest amount of irregular WO_x particles calculated by the Raman (O=W=O + W=O)/W–O–W band intensities ratio was found on the W/Ga(1.09)–γ-Al_2O_3 catalyst. The presence of gallium induced higher activity on the dibenzothiophene hydrodesulfurization reaction in all catalysts tested. The highest Raman ratio and the highest activity were found for the W/Ga(1.09)–γ-Al_2O_3 catalyst, suggesting that better dispersed W species could be responsible for the highest HDS activities.

1. Introduction

The environmental regulations have forced the oil industry to reduce the sulfur content in gas oil cuts and gasolines, which nowadays should contain less than 10 ppm of sulfur for the European market. Such a reduction has implied a great research effort on hydrotreating (HDT) catalysts in the last decades and many approaches to prepare more active catalysts have been considered, such as varying the preparation method, changing the active component, changing the support or other permutations and combinations.

Regarding the nature of the active phase, following the first papers of Pecoraro and Chianelli [1] and Lacroix et al. [2], dealing with the evolution of catalytic properties of transition metal sulfides with their position in the periodic table, many works on ruthenium, rhenium, vanadium, iridium and ternary sulfides have been published and recently reviewed, respectively, by de los Reyes [3], Blanchard et al. [4], Escalona et al. [5], Hubault [6], Vit [7], and Afanasiev and Bezverskhyy [8]. The effect of support in hydrotreating has not been less studied and several reviews [9–11] summarized and discussed variations of catalytic activities due to the support like alumina, titania, zirconia, zeolites and carbon. However, and in spite of such an amount of researches, the commercial HDS catalysts are generally still based on an active phase of molybdenum (Mo) or tungsten (W) promoted by cobalt (Co) or nickel (Ni) and supported over alumina. Nevertheless, it has been rapidly recognized that alumina is not an inert carrier and that the promoter ion (Co or Ni) can react with the support and occupy octahedral or tetrahedral sites in external layers or even form some inactive phase as $CoAl_2O_4$ (or $NiAl_2O_4$). Thus, the amount of promoter involved in the formation of the so-called "CoMoS" ("NiMoS", "NiWS") phase, recognized to be the active phase [12], could be decreasing. Attempt to avoid such a loss of promoter inside the carrier has been the object of numerous studies and many papers reported the influence of additives or modifiers as Mg, Ca, Ti, Fe, Mn or Zn. Unfortunately, most of these approaches have been disappointing and these metals are not suitable for improving HDS activity, excepted by the addition of small amount of Zn as proposed by Martinez and Mitchell [13].

Gallium has been scarcely studied as an additive, but some of us recently reported that Ga^{3+}, added to the alumina support before the impregnation of the active phase, increased the HDS activity of CoMo and NiMo catalysts tested in hydrodesulfurization (HDS)

* Corresponding author at: Universidad A. Metropolitana-Iztapalapa, División de Ciencias Básicas e Ingeniería, Av. FFCC R Atlixco 186, Col. Vicentina, 09340 México, D.F., Mexico. Tel.: +52 5558044603; fax: +52 5556122479.
E-mail addresses: jarh@xanum.uam.mx, toniodlrh@hotmail.com (J.A. de los Reyes).

1381-1169/$ – see front matter © 2010 Elsevier B.V. All rights reserved.
doi:10.1016/j.molcata.2010.03.008

of dibenzothiophene (DBT) and 4,6-dimethyldibenzothiophene [14,15]. It has been suggested that the strong affinity of gallium with the tetrahedral coordination sites of the alumina would decrease the formation of $CoAl_2O_4$ (or $NiAl_2O_4$) entities and therefore, it could lead to a high amount of promoter, able to form the mixed phase. As a continuation of this work, we decided to investigate if such effect could be also observed for NiW-based catalysts. In a first approach, we report here the effect of gallium on the synthesis of γ-Al_2O_3-supported WS_2 catalysts and their activities in DBT HDS reaction. Characterization of alumina carrier after gallium impregnation process was performed by plasma coupled atomic emission spectroscopy (AES-ICP), N_2 physisorption, X-ray diffraction and electrophoretic migration measurements. Calcined WO_x samples supported on alumina modified by gallium were characterized by Raman spectroscopy in order to get insight into tungsten oxide molecular structures.

2. Experimental

2.1. Supports and standards preparation

The supports were prepared by pore filling impregnation of a commercial γ-Al_2O_3, surface area 260 $m^2\,g^{-1}$, pore volume (V_p) 0.66 $cm^3\,g^{-1}$ and particle size 80–120 μm. For each preparation 1 g of the alumina carrier was mixed with an aqueous solution of $Ga(NO_3)_3{\cdot}H_2O$ (Aldrich-Chemical) containing the amount of gallium salt in order to obtain supports with nominal composition of 0, 0.30, 0.60, 0.90, 1.20, 1.60, 1.80 and 2.40 wt.% of metal. After 12 h, the obtained solids were dried at 393 K for 12 h and calcined at 723 K for 4 h under a flow of air (5.16×10^{-3} mol min^{-1}) with a heating rate of 1 K min^{-1}. $GaAl_2O_4$ used as a reference for the Zeta potential experiment was prepared from gallium and aluminium nitrates according to the procedure described by Arean et al. [16].

2.2. Catalysts preparation

In a typical preparation of W catalysts, the support was impregnated with a solution of ammonium metatungstate $(NH_4)_6W_{12}O_{39}{\cdot}H_2O$ from Aldrich at natural pH (3.73). After 12 h, the obtained solids were dried at 393 K for 12 h and calcined at 673 K for 4 h under a stream of air (5.16×10^{-3} mol min^{-1}) with a heating rate of 1 K min^{-1}. The loading of the W was 2.8 atoms per nm^2 of initial surface area of the alumina support.

2.3. Characterization of the solids

Surface area, pore volume, and pore size distribution of the supports were obtained from N_2 adsorption and desorption isotherms using the conventional BET and BJH methods. The samples were first dried at 393 K for 2 h and subsequently outgassed at 573 K under vacuum. Afterwards, the N_2 adsorption measurements were carried out at 73 K. After calcination, the metal contents were determined by plasma coupled atomic emission spectroscopy (AES-ICP) after appropriate dissolution of the solids samples.

Determinations of the Zeta potential were made using an electrophoresis instrument (Zeta-Meter ZM-77) basically constituted by an AO microscope in a Riddick Type II Y UAV cell, with Pt-Ir cathode and a cylindrical Mo anode. The samples were studied using 300 mg of the particles ultrasonically dispersed in 300 mL of 10^{-3} M KCl solution. The pH values were adjusted with 1–3 M HCl or KCl solution. Both, electrophoretic migration rate and Zeta potential are related by the Helmholtz–Smoluchowski equation. As in previous studies [17], Park's definition for zero point charge (ZPC) and isoelectric point (IEP) were used. According with this definition ZPC and IEP are used for mixtures of phases (i.e. Ga(x)–γ-Al_2O_3) and pure phases (i.e. Ga_2O_3 and $GaAl_2O_4$, respectively). Thus the relation between ZPC and IEP values is described by the following equation: $ZPC = \Sigma(IEP)_i \times X_i$, were X_i correspond to superficial molar fraction of each phase [18]. Both the IEP and ZPC values are obtained from at least two determinations of the dependence of the ZP and pH.

Raman spectra were obtained at room temperature on a T64000 triple monochromator (Jobin-Yvon-Horiba) using the 514.5 nm line of an Ar^+ laser (Lexel Laser). All the spectra were obtained at a power of 10 mW at the laser head, in the range 10–1600 cm^{-1}, using an Olympus microscope with an ×100 objective and 10 accumulations of 60s each. The spectrum resolution was 1 cm^{-1}. Gaussian deconvolution of spectra was carried out with appropriate commercial software.

2.4. Catalytic activities measurements

The HDS of DBT was performed in a 500 mL batch reactor, magnetically stirred (1200 rpm) (Parr Instrument Co.) equipped with four baffles on the wall to prevent vortex formation. The conditions of the tests were as follows: temperature of 593 K under a hydrogen atmosphere of 5 MPa for 8 h, using 400 mg of sulfided catalyst and 1.22×10^{-3} mole of DBT dissolved in 100 mL hexadecane (Aldrich-chemical Co.). The reactor was flushed with nitrogen and heated under stirring to reach the reaction temperature, hydrogen was then introduced (P_{tot} = 5 MPa). The reaction time was counted from this moment. The total pressure was controlled constantly during the course of the reaction by adding hydrogen to compensate for its consumption. Samples were periodically collected and analyzed quantitatively by gas chromatography. The catalytic activity was expressed by the initial reaction rate (mol DBT transformed per second and per gram of catalyst).

3. Results and discussion

3.1. Supports characterization

It is known that pH and metal concentration of an impregnating solution and ZPC of the carrier are related to the amount and surface structure of supported metal oxides. Regarding the chemistry of $Ga(NO_3)_3{\cdot}H_2O$ aqueous solutions, equilibria for species at a given Ga concentration can be calculated. Thus, gallium speciation diagrams were obtained for gallium nitrate solutions at two different concentrations by using the Hydra-Medusa [19] software (Fig. 1). These diagrams are in agreement with the literature [20] at standard conditions. For hydrolyzed gallium species diagrams we considered that $Ga_{26}(OH)_{65}{}^{13+}$ polymeric species would be present and they lead to the possible precipitation of traces of solid α-GaOOH.

All calculated Ga speciation diagrams showed three mononuclear Ga-hydroxide species in solution (Ga^{3+}, $GaOH^{2+}$ and $Ga(OH)_2{}^+$) between pH 0 and ∼2.5. At pH values between 2.5 and 6.3, $Ga(OH)_3$ and $Ga_{26}(OH)_{65}{}^{13+}$ polymeric species would be present and they were predominant over the former. Also, we can observe a slight shift to more acidic pH values and a slight increment on the polynuclear hydroxyde amount when the solution concentration increased. Therefore impregnation with solutions at pH higher than ∼2.5 must be avoided. In the case of our series, we found that the experimental pH of gallium aqueous solutions decreased from pH 2.4 to 1.5 for nominal gallium contents between 0.60 and 2.4 wt.%, respectively. Fig. 2 reports some examples of the relationship between the Zeta potential and pH for the sample containing 0.55, 0.84, and for 1.20 wt.% of gallium. For the latter sample two experimental determinations indicate a good reproducibility of the technique. Such curve allows the ZPC of the sample to be determined and values obtained for the different samples Ga(x)–γ-Al_2O_3 are depicted in Fig. 3. The ZPC for the Ga(x)–γ-Al_2O_3 samples

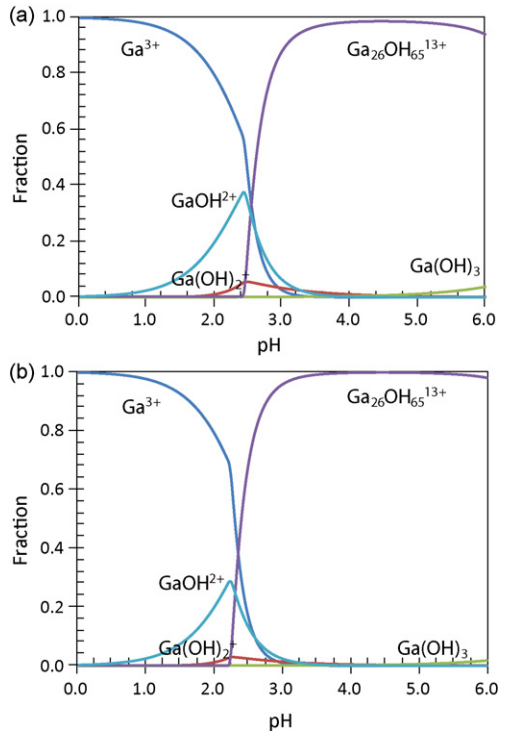

Fig. 1. Hydra-Medusa [17] distribution diagrams of Ga-hydroxide species as a function of gallium concentration for (a) Ga 0.90 wt.% and (b) Ga 2.4 wt.% solutions. Calculated at standard conditions (zero ionic strength), 200 calculation steps.

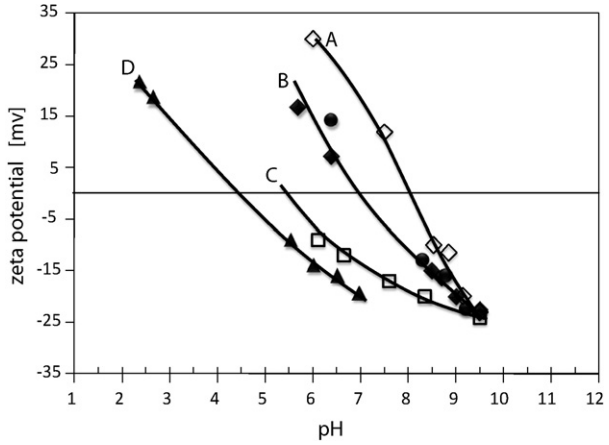

Fig. 2. Zeta potential at 298 K as a function of suspension pH for: (A) Ga(0.55)–γ-Al_2O_3, (B) Ga(1.09)–γ-Al_2O_3, (C) Ga(0.84)–γ-Al_2O_3 and (D) $GaAl_2O_4$.

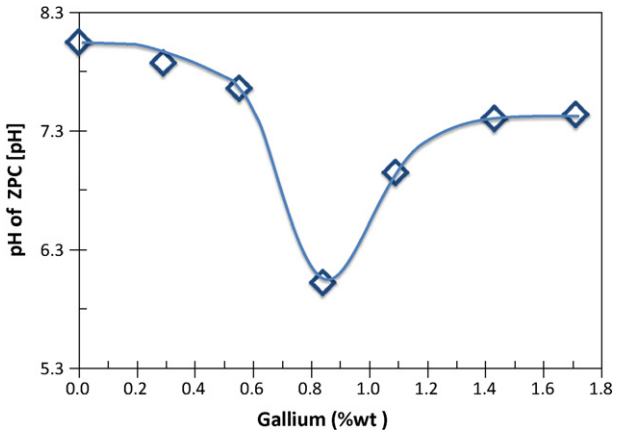

Fig. 3. Variation of the isoelectric point of Ga(x)–γ-Al_2O_3 supports with the Ga content.

decreased when the Ga content increased up to 1% of gallium, then this value increased for higher Ga contents. Such a variation suggests an increase in the quantity of a compound at the alumina surface with an IEP less than 8.0 (IEP of the γ-Al_2O_3.) at low Ga content. Parallel with previous results obtained by Gil Llambias et al. [17] for NiO/γ-Al_2O_3 and CoO/γ-Al_2O_3 systems suggests the formation of some surface spinel as $GaAl_2O_4$. Indeed, the IEP of the synthesized $GaAl_2O_4$ was 4.2 (see Fig. 2) and it could therefore easily explain the decrease of IEP at low Ga content. For Ga concentration higher than 1–1.2 wt.% there is probably formation of Ga_2O_3 on the surface of alumina and the IEP of this compound being close to 9 [21], it could explain the changes in the IEP of the samples.

Such interaction of Ga^{3+} entities with alumina has been early reported by Cimino et al. [22] and Lo Jacono et al. [23]. These authors observed a high affinity of Ga^{3+} to the tetrahedral sites of alumina, modifying the ratio of tetrahedral/octahedral species of Ni ($Ni_{tet}^{2+}/Ni_{oct}^{2}$) in a Ni/γ-$Al_2O_3$ solid. A similar effect was observed when gallium was added to the CoMo catalyst and these authors observed that the $Co_{tet}^{2+}/Co_{oct}^{2}$ ratio changed as a function of the metal loading and of the impregnation sequence. Therefore, our electrophoretic migration studies strongly support the existence of a high interaction between Gallium and Alumina in which the Ga^{3+} ions will occupy superficial tetrahedral sites on the support.

Textural properties for the Ga-impregnated samples after calcination are reported on Table 1 and no significant differences in surface area, average pore diameter and pore volume data were detected, indicating no major modification on the texture of the solids. The plasma coupled atomic emission spectroscopy showed (see Table 1) that the nominal and real Ga wt.% contents were in fair agreement (±10%).

3.2. Catalysts characterization

For the preparation of supported W catalysts a tungsten speciation diagram was obtained (Fig. 4), considering 2.8 atoms of

Table 1
Textural properties and chemical analysis of prepared supports.

Support	A_{BET} ± 6 m^2 g^{-1}	d_p (Å) ± 3%	V_p (cm^3 g^{-1}) ± 5%	AES-ICP wt.% Ga
γ-Al_2O_3	260	109	0.66	–
0.30 wt.% Ga	–	–	–	0.29
0.60 wt.% Ga	248	98	0.55	0.55
0.90 wt.% Ga	245	98	0.54	0.84
1.20 wt.% Ga	240	98	0.53	1.09
1.50 wt.% Ga	–	–	–	1.43
1.80 wt.% Ga	238	95	0.51	1.71
2.40 wt.% Ga	235	94	0.48	2.22

A_{BET}, surface area (m^2 g^{-1}); d_p, pore diameter (Å); V_p, pore volume (cm^3 g^{-1}); AES-ICP, plasma coupled atomic emission spectroscopy

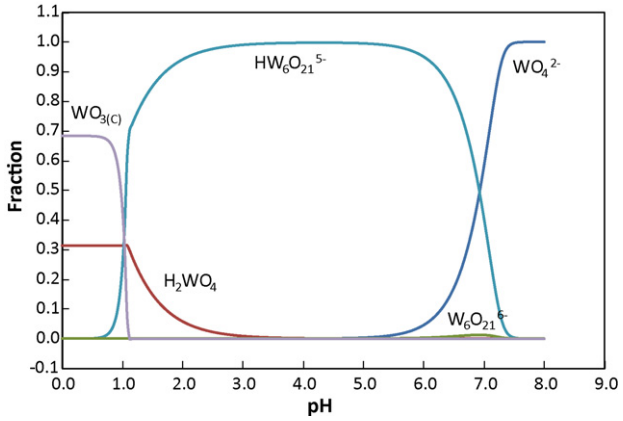

Fig. 4. Hydra-Medusa [17] distribution diagrams of W-hydroxide species as a function of tungsten concentration $[WO_4^{2-}]_{TOT}$ = 1.21 mM, calculated at standard conditions (zero ionic strength), 200 calculation steps.

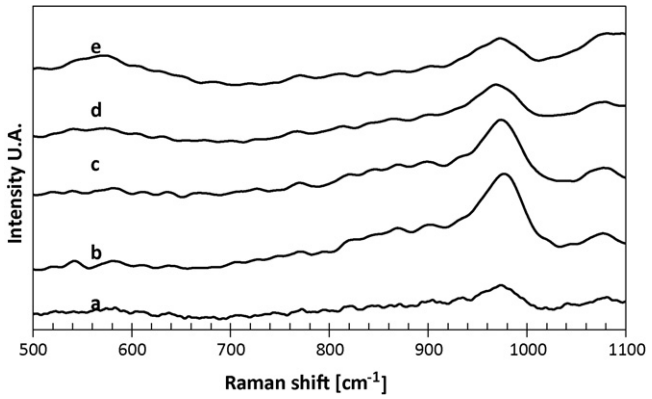

Fig. 5. Raman spectra of calcined $WO_x/Ga(x)$–γ-Al_2O_3 catalysts. (a) WO_x/γ-Al_2O_3, (b) WO_x/Ga(0.84)–γ-Al_2O_3, (c) WO_x/Ga(1.09)–γ-Al_2O_3, (d) WO_x/Ga(1.71)–γ-Al_2O_3 and (e) Ga(2.2)–γ-Al_2O_3.

W nm^{-2} equivalent to $[WO_4^{2-}]_{TOT}$ = 1.21 mM. Fig. 4 showed the presence of five tungsten hydroxide species ($WO_{3(C)}$, H_2WO_4, $HW_6O_{21}^{5-}$, $W_6O_{21}^{6-}$ and WO_4^{2-}) at that concentration. We found the experimental pH for the ammonium metatungstate ($(NH_4)_6W_{12}O_{39}{\cdot}H_2O$) solution to be 3.73. At that pH only the anionic $HW_6O_{21}^{5-}$ species is present. If all the Ga–γ-Al_2O_3 materials had the same IEP, the interaction between the support and W-hydroxide anionic species ($HW_6O_{21}^{5-}$) could lead to the formation of the same type of WO_x structures at the surface for all catalysts. However, results from electrophoretic analysis of supports after Ga impregnation and calcination indicated different IEP and thus, the interaction of the modified carrier with the anionic species ($HW_6O_{21}^{5-}$) was different depending on the Ga content. $WO_x/Ga(x)$–γ-Al_2O_3 calcined samples were therefore characterized by Raman spectroscopy in order to gain insight about this matter.

Raman spectrum for the carrier before impregnation exhibited broad weak peaks at ~573 and 1080 cm^{-1} (expanded scale spectra not shown here) probably related with the gamma alumina phase. The supports with different gallium contents also showed this low-intensity peak. Raman bands for amorphous Ga_2O_3 reference sample were not observed in agreement with previous results reported by Olorunyolemi and Kydd [24]. Thus, no peaks were found for the Ga(x)–γ-Al_2O_3 solids.

Before the presentation of results on supported tungsten catalysts, it seems necessary to remember some experimental considerations about tungsten oxide compounds. Crystallographic studies have shown that WO_3 has various stable phases with more or less distorted ReO_3-like structures. At room temperature, the monoclinic phase is favoured [25]. The Raman spectrum of monoclinic WO_3 is composed of several peaks in the region 20–350 cm^{-1} and two intense peaks at 717 and 807 cm^{-1} assigned to W=O stretching modes [26,27]. The main difficulty for the interpretation of the Raman spectrum is that this region has been found very sensitive in particular to dehydration, hydration and to surface concentration of the supported oxide [28]. As mentioned by Horsley et al. [27], the position of the highest band reflects the highest bond order present in the tungsten oxide structures. In that sense, tetrahedral groups would present Raman bands at higher frequency than octahedral groups. Moreover, distorted structures of these groups can increase the W–O bond order and complicate the distinction between tetrahedral and octahedral groups based on band position.

Raman spectra for the $WO_x/Ga(x)$–γ-Al_2O_3 calcined series showed a broad Raman band in the region 740–1060 cm^{-1} related with WO_x species [29–35] (Fig. 5). An appropriate analysis of this band and in agreement with prior work revealed that this peak can be fitted considering four specific peaks. A signal between ~970 and 1000 cm^{-1} arising from the symmetric stretching vibrations of the terminal W=O bonds in octahedral polytungstate species [31,32,34–36]. A second peak between ~940 and 950 cm^{-1} can be related to the same vibrational mode but it could be assigned to tetrahedral coordinated monotungstate species [31–34,36]. Monotungstate species exhibit dioxo structures (O=W=O) in a WO_4 coordination and polytungstates have probably monoxo (W=O) structures in octahedral coordination [31,36]. The weak broad band at 805 cm^{-1} is related with W=O stretching mode of WO_3 microcrystallites [31–34,36]. An additional Raman band was also observed at 880 cm^{-1}. This band has been generally observed at low WO_x covering [33,35,37] as occurs with our samples. The position of this band is too low for the stretching mode of the WO_4 coordination, Vuurman and Wachs [35] proposed that this Raman band comes from a second surface tungstate species with an octahedral coordination. This band is assigned to the asymmetric stretching of W–O–W linkage, in the case of distorted tetrahedral coordinated tungsten oxide where a fraction of the species are in a dimeric form [27] or surface tungsten oxide species at low polymerization [37].

Assuming the existence of these four bands the expanded scale spectra of tungsten catalysts were deconvoluted. An example of deconvolution is shown in Fig. 6.

For the $WO_x/Ga(x)$–γ-Al_2O_3 calcined samples, variations in the intensities of peaks in the region ~950–1000 cm^{-1} were observed with respect to the gallium content. This effect was more rele-

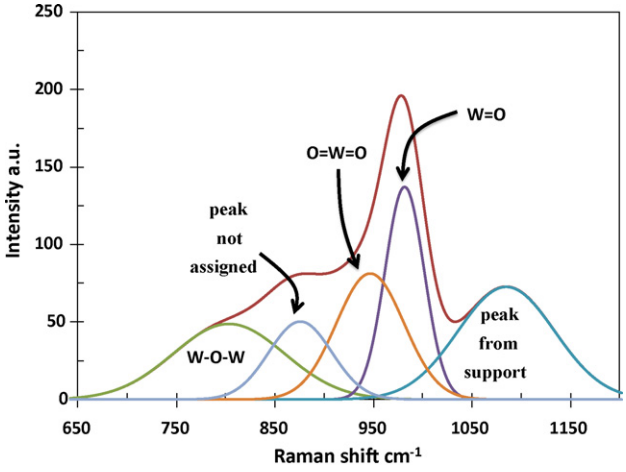

Fig. 6. Gaussian deconvolution example of $WO_x/Ga(0.84)$–γ-Al_2O_3 spectrum.

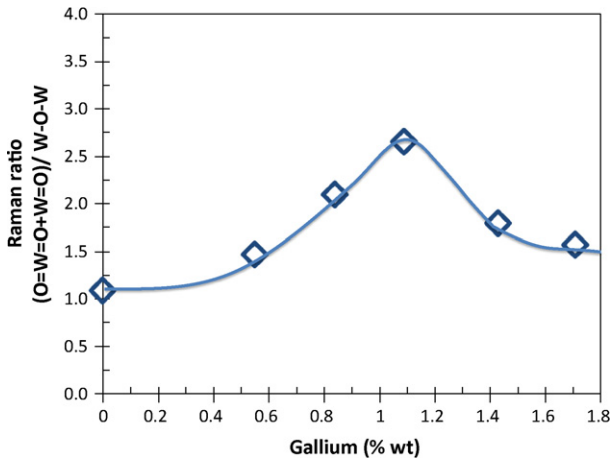

Fig. 7. Raman ratio (O=W=O + W=O)/W–O–W as a function of the Gallium content in the WO_x catalysts.

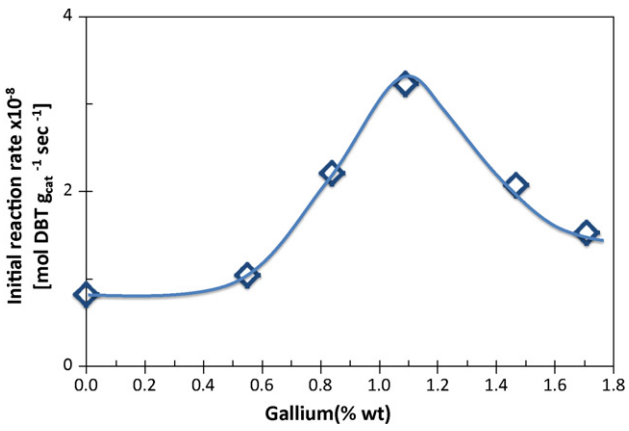

Fig. 8. Catalytic activity of WS_x/Ga(x)–γ-Al_2O_3 catalyst on HDS of DBT. Reaction in a batch reactor at 593 K and 800 psi. Catalysts were sulfided at 673 K.

vant at low gallium content. In order to obtain information about the structure in different catalysts, the ratio of integrated peak areas by Gaussian deconvolution of terminals bonds (O=W=O and W=O) and internal W–O–W bonds was considered [33,38]. It has been proposed that this ratio suggests a relative measurement of the dispersion of WO_x species [36]. Fig. 7 shows the Raman ratios (O=W=O + W=O)/W–O–W for the WO_x/Ga(x)–γ-Al_2O_3 calcined catalysts. The intensity ratio gradually increased from 1.08 in the gallium free sample to 1.46, 2.09 and 2.6 for the catalysts with 0.55, 0.84 and 1.09 wt.% Ga, respectively. After the maximum ratio was reached for the catalyst WO_x/Ga(1.09)–γ-Al_2O_3, the ratio decreased to 1.79, 1.56 and 1.69 for the samples supported on carriers containing 1.43, 1.71 and 2.22 wt.% Ga, respectively. It seems that the ratio reached a constant value at high gallium contents. The rise in the intensity ratio shows that the terminal W=O species became more abundant than the W–O–W internal bonds as the gallium content increased. A relative higher amount of W=O bonds on the structure for WO_x solids supported on alumina containing 0.84 and 1.09 wt.% Ga than in the free gallium sample suggests the presence of highly distorted tetrahedral and octahedral WO_x species [30,35,38].

The increase in the Raman ratio for the catalysts indicated that the gallium incorporation on the Ga-modified alumina support had an important effect on the structure formation of WO_x species. The presence of structures with a higher amount of W=O bonds probably means a better dispersion.

The modification of alumina superficial properties by Ga exhibited a clear effect on the formation of WO_x structures. It is well known that there exist different charges for superficial species that depend on the IEP. The net surface charge is preferably positive at pH less than the IEP and preferably negative at pH higher than that [30,39]. In our study the ammonium metatungstate impregnation solution at pH 3.73 was used for all materials. At this pH value, the support was positively charged and the $HW_6O_{21}{}^{5-}$ anions adsorption was highly favoured. Also it could be considered that the interaction between the impregnation solution and the different materials may result in a new modification or shift of the IEP for the W oxide supported catalysts.

3.3. Catalytic activities

The influence of gallium content in the W sulfide catalysts on the DBT HDS reaction is shown in Fig. 8. The activity displayed a volcano curve, thus activity increased with Ga content and reached a maximum for the WS_2/Ga(1.09)–γ-Al_2O_3 sample. Then an activity decrease was noticed for higher Ga concentration. These results reveal that gallium improved the activity of the W-based catalysts. The DBT transformation rate over the catalysts 0.84, 1.09 and 1.43 wt.% Ga showed 17%, 59% and 25%, respectively, higher activity than the W reference catalyst (without Ga). Further increase in the gallium content led to a decrease in activity.

The selectivities for all main products (biphenyl ~60%, cyclohexylbenzene ~20%) are almost the same for all tested catalysts. Cracking products such as benzene, cyclohexane and cyclohexenes were also detected (accounting for ca. 20%). However, no other products coming from further cracking of these molecules were observed. These selectivity data pointed out to some acidity on the solids. Appropriate characterization is in progress in order to deal with this issue. The presence of tetrahydrodibenzothiophene and bicyclohexyl was not detected.

The behaviour depicted in Fig. 8 is similar to that early published by Altamirano et al. [14,15] although the present paper deals with unpromoted W catalysts. Our results confirm clearly a positive effect of Ga on the HDS activity for WS_2 catalysts. Furthermore, there is a parallel between the activity curve and the Raman ratio (O=W=O + W=O)/W–O–W results, suggesting a relationship between better dispersed WO_x surface species, leading to more active WS_2 catalysts.

As mentioned before, some of us reported that small amounts of Ga (0.60 wt.%) increased the HDS activity of alumina supported NiMo and CoMo materials [15]. It was found that a change in the promoter (Co^{2+} or Ni^{2+}) interaction with the carrier is induced by the affinity of gallium at low loadings for the tetrahedral sites of alumina, leading to an increase in the octahedral species of Ni or Co. These modifications were ascribed to the improvement of the HDS activity. However in this work, the maximum activity value was found for the W catalyst supported on the 1.09 wt.% Ga material and since we are dealing with unpromoted W catalyst different interactions for Ga with W species should be considered. Therefore, it is clear that Ga improved the dispersion of W species in the oxidic state and Ga addition may modify the properties of the sulfided phases. Characterization work is in progress to support such a conclusion.

4. Conclusions

The electrophoretic study indicated that Ga addition affected significantly the surface of alumina. The presence of at least two gallium species was proposed, at low gallium content $GaAl_2O_4$ species decreased the IEP and probably the formation of Ga_2O_3 at higher contents increased again the IEP. Raman spectroscopy showed the gallium incorporation had a strong effect in the formation of WO_x species at the surface of catalysts. The presence of gallium induced

to higher activities on the DBT HDS reaction for all Ga-containing catalysts. The highest Raman (O═W═O + W═O)/W–O–W band intensities ratio and the highest activity were found for the W/Ga(1.09)–γ-Al_2O_3 catalyst, suggesting that better dispersed W species could be responsible for the highest HDS activities.

Acknowledgements

J.N. Díaz de León H. expresses his gratitude to CONACyT and the France-México Postgraduate Cooperation Program for the scholarships.

References

[1] T.A. Pecoraro, R.R. Chianelli, J. Catal. 67 (1981) 430.
[2] M. Lacroix, N. Boutarfa, C. Guillard, M. Vrinat, M. Breysse, J. Catal. 120 (1989) 487.
[3] J.A. de los Reyes, Appl. Catal. A 322 (2007) 106.
[4] J. Blanchard, K.K. Bando, T. Matsui, M. Harada, M. Breysse, Y. Yoshimura, Appl. Catal. A 322 (2007) 98.
[5] N. Escalona, M. Vrinat, D. Laurenti, F.J. Gil Llambias, Appl. Catal. A 322 (2007) 113.
[6] R. Hubault, Appl. Catal. A 322 (2007) 121.
[7] Z. Vit, Appl. Catal. A 322 (2007) 142.
[8] P. Afanasiev, I. Bezverskhyy, Appl. Catal. A 322 (2007) 129.
[9] F. Luck, Bull. Soc. Chim. Belg. 108 (1991) 781.
[10] M. Breysse, J.L. Portefaix, M. Vrinat, Catal. Today 10 (1991) 489.
[11] M. Breysse, P. Afanasiev, C. Geantet, M. Vrinat, Catal. Today 86 (2003) 5.
[12] H. Topsoe, R. Candia, N.-Y. Topsoe, B.S. Clausen, Bull. Soc. Chim. Belg. 93 (1984) 783.
[13] N.P. Martinez, P.C.H. Mitchell, in: H.F. Barry, P.C.H. Mitchell (Eds.), Proceedings of the 3rd Climax International Conference on the Chemistry and Uses of Molybdenum, Climax Molybdenum, Ann Arbor, MI, 1979, p. 105.
[14] E. Altamirano, J.A. de Los Reyes, F. Murrieta, M. Vrinat, J. Catal. 235 (2005) 403.
[15] E. Altamirano, J.A. de Los Reyes, F. Murrieta, M. Vrinat, Catal. Today 133–135 (2008) 292.
[16] C. Arean, M. Delgado, V. Montouillout, D. Massiot, Zeitschrift fuer Anorganische und Allgemeine Chemie 63 (2005) 2122.
[17] F.J. Gil Llambias, A.M. Escudey-Castro, J. Santos Blanco, J. Catal. 83 (1983) 225.
[18] G.A. Parks, Adv. Chem. Ser. 67 (1967) 121.
[19] I. Puigdomenech, Hydra-Medusa software. (Hydrochemical Equilibrium Constant, Database and Make Equilibrium Diagrams Using Sophisticated Algorithms), Inorganic Chemistry, Royal Institute of Technology, Stockholm, Sweden, 2004.
[20] S.A. Wood, I.M. Samson, Ore Geol. Rev. 28 (2006) 57.
[21] M. Kosmulski, J. Colloid Interface Sci. 238 (2001) 225.
[22] A Cimino, M. Lo Jacono, M. Schiavello, J. Phys. Chem. 79 (1975) 243.
[23] M. Lo Jacono, M. Schiavello, V.H.J. De Beer, G. Minelli, J. Phys. Chem. 81 (1977) 16.
[24] T. Olorunyolemi, R.A. Kydd, Catal. Lett. 65 (2000) 185.
[25] M.F. Daniel, B. Desbat, J.C. Lassegues, B. Gerand, M. Figlarz, J. Solid State Chem. 67 (1987) 235.
[26] E. Haro-Poniatowski, M. Jouanne, J.F. Morhange, C. Julien, R. Diamant, M. Fernández-Guasti, G.A. Fuentes, J.C. Alonso, Appl. Surf. Sci. 127–129 (1998) 674.
[27] J.A. Horsley, I.E. Wachs, J.M. Brown, G.H. Via, F.D. Hardcastle, J. Phys. Chem. 91 (1987) 4014.
[28] S.S. Chan, I.E. Wachs, L.L. Murrell, L. Wang, W. Keith, J. Phys. Chem. 88 (1984) 5831.
[29] A. Scholz, B. Schnyder, A. Wokaun, J. Mol. Catal. A 138 (1999) 249.
[30] I.E. Wachs, Characterization of Catalytic Materials, Butterworth–Heinemann, 1992.
[31] I.E. Wachs, T. Kim, E.I. Ross, Catal. Today 116 (2006) 162.
[32] M.L. Hernández, J.A. Montoya, I. Hernández, M. Viniegra, M.E. Llanos, V. Garybay, P. del Angel, Micropor. Mesopor. Mater. 89 (2006) 186.
[33] D. Barton, M. Shtein, R. Wilson, S. Soled, E. Iglesia, J. Phys. Chem. B 103 (1999) 630.
[34] T. Kim, A. Burrows, C. Kiely, I. Wachs, J. Catal. 246 (2007) 370.
[35] M.A. Vuurman, I.E. Wachs, J. Phys. Chem. 96 (1992) 5008.
[36] S.D. Kohler, J.G. Ekerdt, D.S. Kim, I.E. Wachs, Catal. Lett. 16 (1992) 231.
[37] D.S. Kim, M. Ostromecki, I.E. Wachs, J. Mol. Catal. A 106 (1996) 93.
[38] T.A. Zepeda, B. Pawelec, A. Olivas, J.L.G. Fierro, Mater. Res. Innov. 11 (2007) 54.
[39] J. Cruz, M. Avalos, R. López, M.A. Bañares, J.L. Fierro, J.M. Palacios, A. López, Appl. Catal. A 224 (2002) 97.